# Motion Tracking on Elbow Tissue from Ultrasonic Image Sequence for Patients with Lateral Epicondylitis

Yuh-Hwan Liu, Shu-Min Chen, Chi-Yi Lin, Chung-I Huang, Yung-Nien Sun

Abstract—In this study, Kinesio Tape® is used in patients with lateral epicondylitis. The ultrasonic image sequences of elbow are recorded dynamically, and then motion tracking is applied to assist in understanding the effect of the therapy. Motion tracking, based on optical flow method, is used to track certain landmark on the ultrasound image, which is very ambiguous, for estimating the motion of muscle. Hierarchical block tracking technique is proposed to perform this task. The motions with and without Kinesio Taping are compared and can be used as quantitative indicators for the treatment. The experimental results show that Kinesio Taping makes the motion of muscle on the ultrasonic images enlarge. It means that the performance of muscle motion gets improve.

### I. INTRODUCTION

inesio Tape<sup>®</sup> exhibits its effect through the activation of neurological and circulatory systems with movement. The tape is used in a variety of setting for edema reduction, pain management, inhibition and facilitation of motor activity. The basic principle of therapeutic taping for weakened muscle contractions is to wrap the tape around the affected muscle in the direction from the origin to insertion of muscle, as shown in . The muscle is placed on gentle functional stretch with application of the tape at 10% of its resting static length [1]. Recently, Kinesio Taping has been used for reducing pain related to musculo-skeletal injuries, this has led to its frequent use in many exercises and sport related scenes. It has also been thought that Kinesio Taping could improve sports performance based on muscular functions [2]. Several clinical parameters are measured for evaluating the therapy effect of Kinesio Taping, such as the difference of the maximal isometric force (MIF) for the elbow in a 90 degree angle, range of motion (ROM) of the elbow joint, the pain

Manuscript received April 2, 2007. This work was supported in part by the Taiwan National Science Council under Grant NSC-95-2221-E-006-239 -MY2.

Yuh-Hwan Liu is with the Department of Information Management, Chia-Nan College of Pharmacy & Science, Tainan, Taiwan. (phone: 886-6-3662019; fax: 886-6-3660607; e-mail: <a href="mailto:qlyh@mail.chna.edu.tw">qlyh@mail.chna.edu.tw</a>).

Shu-Min Chen is with the Department of Physical Medicine and Rehabilitation, College of Medicine, National Cheng-Kung University, Tainan, Taiwan. (e-mail: <a href="mailto:chengsm@mail.ncku.edu.tw">chengsm@mail.ncku.edu.tw</a>).

Chi-Yi Lin is with the Visual System Laboratory, Department of Computer Science and Information Engineering, National Cheng-Kung University, Tainan, Taiwan. (e-mail: <a href="mailto:chiyilin.o@gmail.com">chiyilin.o@gmail.com</a>).

Chung-I Huang is with the Visual System Laboratory, Department of Computer Science and Information Engineering, National Cheng-Kung University, Tainan, Taiwan. (e-mail: <a href="mailto:schumi@vision.csie.ncku.edu.tw">schumi@vision.csie.ncku.edu.tw</a>).

Yung-Nien Sun is with the Visual System Laboratory, Department of Computer Science and Information Engineering, National Cheng-Kung University, Tainan, Taiwan. (e-mail: <a href="mailto:ynsun@mail.ncku.edu.tw">ynsun@mail.ncku.edu.tw</a>).

scale (during extension, flexion, and pressure), circumference of the brachium, plasma levels of creatin kinase (CK) from the blood. An ultrasound diagnoses, using a B mode ultrasound device to measure muscle thickness and signal intensity of the brachium flexor group, was also used by the clinicians to observe the musculo-skeletal changes during the treatment [2].

However, there are deficient researches in quantitatively analyzing the ultrasound of elbow that might help us to understand the mechanisms of the Kinesio Taping. The motion of the extensor carpi radialis muscles, a quantitative measurement, is interested in our study.



Fig. 1 The direction of the taping is from the origin to insertion of the affected muscle.

### II. MATERIALS AND METHODS

### A. Subjects and Procedure

Two volunteers who had slightly lateral epicondylitis were used as subjects. The initial position of the wrist is in the flexing movement. The subjects performed passive and active movements by extending and flexing the wrist in two seconds per period with and without Kinesio Taping. The dynamic ultrasonic image sequences, longitudinal scans on the position about one-inch below the lateral epicondyle of the humerus, are acquired in each movement at the time points before taping, just after taping, taping after 24 hours, and just removing tape. The terason t3000 ultrasound system, a portable PC-based ultrasound imaging equipment, is used to acquire the dynamic ultrasonic image sequences with image resolution 469x367 and 65 frame numbers.

### B. Motion Tracking

Muscle in ultrasound image lacks observable landmarks so

that the movement estimation becomes difficult. The motion tracking, based on the optical flow method, uses the hierarchical block tracking technique to trace the time variant texture object with highly similarity. The motion between two image slices is first estimated by the hierarchical feature weighted method [3]. The hierarchical block tracking method is based on a fine-to-coarse approach. In this method, the motion estimated image pyramid is built at the tracking region. The motion fields are incrementally updated level by level. The motion field on the upper most level of the motion estimated image pyramid represents the total motion effect within the tracking region. Then, the center of the tracking region is moved according the motion field, and the image pyramid on the second slice is built. These steps are repeated until all image slices are processed. The track of the moving object is then obtained.

The hierarchical feature weighted method for optical flow estimation contains three steps and described as follows.

1) Motion Estimation Using Block-matching Algorithm
In the block-matching algorithm, each estimated location
in a processing frame corresponds to a best-matched location
within the search window in the reference frame.

Let  $a_i$  and  $b_i$  represent the vector for all intensities of the processing and the reference matching blocks displaced by the corresponding motion vector  $v_i = (u_i, v_i)$ , respectively. According to the maximum likelihood method for parameter estimation [4]–[5], the optimal estimate of  $v_i$ ,  $\hat{v}$ , is obtained by maximization for each i of the following conditional probability density function:

$$\hat{v} = \arg\max_{v_i} p(a_i \mid b_{i,v_i}) \tag{1}$$

In general cases, the noise assumption is usually made that  $a_i=b_i+n_i$ , where  $n_i$  is a noise process independent of  $b_i$ . If  $p_n(n)$  is the probability density function of each element of the vector  $n_i$ , the maximization of (1) is equivalent to the maximization of (2):

$$\hat{v} = \arg\max_{v_i} \prod_{j=1}^{k} p_n (a_{ij} - b_{ij_i})$$
 (2)

where i is the index of corresponding positions in the search window, and j is the index of pixels in the matching block with size k. If n is a generalized zero-mean Gaussian noise, the maximization of (2) is equivalent to the minimization of the following objective function [4]:

$$\hat{v} = \arg\max_{v_i} \sum_{j=1}^{k} |a_{ij} - b_{ij}|^c$$
 (3)

The most commonly used objective functions are those corresponding to c=1 and c=2, i.e., sum of absolute difference (SAD) and sum of squared difference (SSD), respectively. Both SAD and SSD are designed for minimizing the displaced pixel differences, and the corresponding  $v_i$  with the minimum SAD or SSD is selected as the resulting motion vector. Although SSD penalizes large pixel differences more heavily, the SAD is the most popular

objective function because of its simplicity and fast computation time.

Ultrasonic B-mode images are assumed to be contaminated with multiplicative Rayleigh noise [6]–[7], and a specific design for this case has also been proposed. The maximization of (1) was derived as:

$$\hat{v} = \arg\max_{v_i} \prod_{j=1}^{k} \left\{ \frac{2(a_{ij}/b_{ij})^2}{[(a_{ij}/b_{ij})^2 + 1]^2} \right\}$$
 (4)

The first problem in block-matching algorithms is to decide the size of the matching block and the search window [8]. A large matching block holds more spatial information but loses its local properties. A small block size maintains its local properties but may lead to the aperture problem and be sensitive to noises.

### 2) Hierarchical Maximum a posteriori (MAP) Motion Estimation

To reduce the computational complexity of the full search block-matching algorithm, several fast algorithms have been proposed. Some techniques reduce the computation time by reducing the number of search positions [9]–[10], and others reduce the cost of the matching computation for each search position [11]. Often a hierarchical method [12]–[14] is adopted to further improve efficiency. The hierarchical block-matching algorithm is based on a coarse-to-fine scheme.

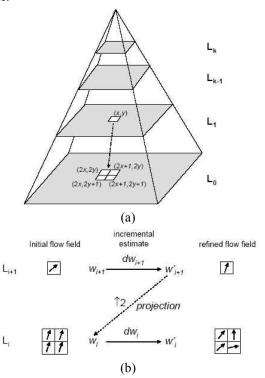


Fig. 2 (a) Image pyramid structure of hierarchical block-matching algorithm, and (b) the multi-resolution incremental motion vector estimation.

Assuming that the processing image is of size  $N \times M$ , an image pyramid of L is shown in Fig. 2 (a) It can be defined as a sequence of image levels  $\{L_0, L_1, \dots, L_{k-1}^{I}, L_k\}$ , where k+1

image levels in total have to be built. The resolution superscript will span from 0 for the finest resolution to k for the coarsest one. In this pyramid structure,  $L_0$  is the original image and  $L_{i+1}$  is a reduced resolution image of  $L_i$ . The reduction process can be formed by successively operating over  $2 \times 2$  neighboring pixels on the lower levels. The block matching algorithm is then performed on the corresponding image pyramids based on a top-down strategy. The motion fields can be incrementally refined level by level, as illustrated in Fig. 2 (b).

The search window can be limited because a small displacement vector in a higher level represents a large one in a lower resolution. Thus, the matching computation throughout the pyramid hierarchy becomes much more efficient, and the large displacement and aperture problems are also reduced.

## 3) Vector Post-Processing Using Adaptive Feature Weighted Filtering

Motion vectors associated with the same object should be similar, resulting in motion smoothness between neighboring pixels. Therefore, the motion vector can be more robustly estimated if the global motion trend of the entire neighborhood is considered. Thus, a motion vector may generally be re-estimated from the motion vectors surrounding it. In this case, the projected motion vector can be computed by the following weighting operator:

$$v_{i=(x,y)}^{l} = \sum_{i' \in Q(x/2,y/2)} w^{l+1} \times v_{i'}^{l+1}$$
 (5)

where image block Q is the filtering mask centered at image position (x/2,y/2) in pyramid level l+1, and  $v_i^{l+1}$  represents the corresponding motion vectors. The weighting factors  $w_i^{l+1}$  are normalized such that the sum of weights is equal to 1. The weighted sum of motion vectors is the projected motion vector that propagates to the next finer level l.

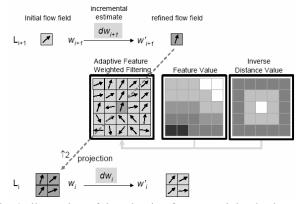


Fig. 3 Illustration of the adaptive feature weighted scheme.

In general, feature areas such as edges and object boundaries provide much more reliable motion information than homogeneous (featureless) areas. Therefore, feature values that can be regarded as a confidence measure should be taken into account in the weighting function.

In this study, motion estimation is based on the

assumptions that the motion field varies smoothly within the tissue region and that the motion estimates at feature pixels are much more reliable. Consequently, the weighting mechanism involves two terms: one captures the influence of feature characteristics, and the other preserves the smoothness property by incorporating an inverse distance constraint. This weighting process can be illustrated in Fig. 3.

We now propose to preserve the smoothness property by using an inversely distance-weighted constraint in the motion estimation. Based on the assumption that the tissue motion field is continuous, the motion vector being estimated is strongly influenced by the motion vectors on the nearby tissues, but is less influenced by those of the tissues further away. Hence, the influence of neighboring regions on each other for estimating the motion field should be inversely related to their distance. Therefore, for each pixel in the image pyramid, the weighting factor in (5),  $w_i^{l+1}$ , is designed to include both the local statistics,  $\alpha$ , and the inverse distance factor. This weighting process is performed on a fixed running window with the weights adaptively adjusted according to the local statistics. The weights in the filtering mask are defined as:

$$w_{i}^{l+1} = g_{1} \times \frac{1/((d_{i}^{l+1})^{a} + b)}{\sum_{i \in O} 1/((d_{i}^{l+1})^{a} + b)} + g_{2} \times \frac{\alpha_{i}^{l+1}}{\sum_{i \in O} \alpha_{i}^{l+1}}$$
(6)

where  $g_1$  and  $g_2$  are scalar parameters, Q is the filtering mask, d is the distance from the image pixel to the center of the filtering mask, and  $\alpha$  is the local variance-to-mean ratio. In (6), the first term is an inverse distance weighted parameter. The parameter a defines the relative influence of the distance terms. The parameter b is given a small value to avoid the problem caused by a zero distance. The second term is a feature weighted value dependent on the variance-to-mean ratio of the image pixel. When the value is large, the corresponding pixel very likely belongs to some apparent structural elements, such as an object boundary, and is thus highly weighted. If the value is small, the corresponding pixel may belong to a homogeneous region and hence the motion vector is less reliable due to the aperture problem. It receives a lower weight for motion propagation.

### III. EXPERIMENTAL RESULTS AND DISCUSSION

The longitudinal scan of extensor carpi radialis muscles is shown in Fig. 4 (a). The left hand side is the proximal part of the muscle near the origin and the right hand side is the distal part. The motion direction is almost parallel to the fiber direction of muscle. The motion direction of muscle is from right to left in the extending movement, while is from left to right in the flexing movement. The thickness of muscle is inconsistent due to the anatomical structure, so that the motion of muscle should be condensed on the left hand side. To prevent from mis-tracking, the tracking region of muscle

should be located at upper part of the image. Four muscle tracking regions are selected on the upper right part of the muscle area, as shown in Fig. 5. To avoid overlapping display of four traces, each trace is display at different *y*-position. The proposed motion tracking method can well trace the motion object, as shown in Fig. 5 (a), while the results obtained by traditional correlation method are not good, as shown in Fig. 5 (b). Since the initial position of the wrist is in the flexing movement, the motion begins in the direction from right to left, i.e. *x*-axis is in the decreasing direction. It is observable that the motion in the extending movement after taping 24 hours is smaller than that before taping. It can be explained as that the muscle motion is constrained by the taping. Therefore, the experimental results are reasonable and can be used as an indicator to evaluate the performance of the muscle.

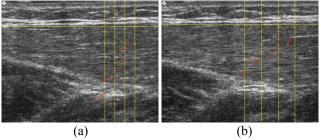


Fig. 4 (a) The ultrasonic image of extensor carpi radialis muscles. The left hand side is the proximal part of the muscle near the origin and the right hand side is the distal part. Four muscle tracking regions, indicated at the yellow dot, are selected on the upper right part of the muscle area. (b)

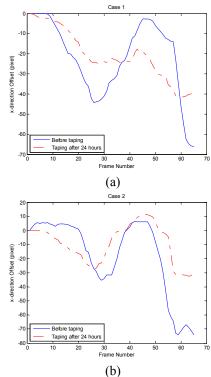


Fig. 5 The average motion of the four tracked regions at the time points before taping and taping after 24 hours. (a) case 1, (b) case 2.

### IV. CONCLUSION

In this study, a new motion tracking algorithm, called hierarchical block tracking, is proposed, and can successfully trace the time variant texture object with high similarity. The hierarchical scheme make it be more flexibility. The proposed tracking method is based on the hierarchical feature weighted block matching, and can obtain more reasonable results than the traditional correlation method. The motion of the extensor carpi radialis muscles can be tracked on the ultrasonic image sequences. And the experimental results show that the motion in the extending movement after taping 24 hours is smaller than that before taping. It is reasonable results in clinical, since the motion of muscle is constrained by the taping.

### REFERENCES

- D. J. Osterhues, "The use of Kinesio Taping<sup>®</sup> in the management of traumatic patella dislocation. A case study," *Physiotherapy Theory* and Practice, Vol. 20, pp. 267-270, 2004.
- [2] K. Nosaka, "The Effect of Kinesio Taping on Muscular Micro-Damage Following Eccentric Exercises," 15th Annual Kinesio Taping International Symposium Review, pp. 70-73, 1999.
- [3] C. H. Lin, C. J. Mark Lin and Y. N. Sun, "Ultrasound motion estimation using a hierarchical feature weighting algorithm," *Computerized Medical Imaging and Graphics*, vol. 31, Issue 3, pp. 178-190, April 2007
- [4] M. G. Strintzis, and I. Kokkinidis, "Maximum Likelihood Motion Estimation in Ultrasound Image Sequences," *IEEE Signal Processing Letters*, Vol. 4, No. 6, pp. 156-157, 1997.
- [5] B. Cohen, and I. Dinstein, "New Maximum Likelihood Motion Estimation Schemes for Noisy Ultrasound Images," *Pattern Recognition*, vol. 35, pp. 455-463, 2002.
- [6] C. B. Burckhardt, "Speckle in ultrasound B-mode scans," *IEEE Trans. on Sonics and Ultrasonics*, vol. 25, no. 1, pp. 1-6, 1978.
- [7] G. E. Sleefe and O. Lele, "Tissue characterization based on scatterer number density estimation," *IEEE Trans. on Ultrasonics Ferroelectrics and Frequency Control*, vol. 35, no. 6, pp. 749-757, 1988
- [8] H. Liu, T. H. Hong, M. Herman, T. Camus, and R. Chellapa, "Accuracy vs Efficiency Tradeoffs in Optical Flow Algorithms," *Computer Vision and Image Understanding*, Vol. 72, No. 3, pp. 271-286, 1998.
- [9] C. H. Lee, and L. H. Chen, "A Fast Motion Estimation Algorithm Based on the Block Sum Pyramid," *IEEE Trans. on Image Processing*, Vol. 6, No. 11, pp. 1587-1590, 1997.
- [10] Y. S. Chen, Y. P. Hung, and C. S. Fuh, "Fast Block Matching Algorithm Based on the Winner-Update Strategy," *IEEE Trans. on Image Processing*, vol. 10, no. 8, pp. 1212-1222, 2001.
- [11] W. Li, and E. Salari, "Successive Elimination Algorithm for Motion Estimation," *IEEE Trans. on Image Processing*, Vol. 4, No. 1, pp. 105-107, 1995.
- [12] K. M. Nam, J. S. Kim, R. H. Park, and Y. S. Shim, "A Fast Hierarchical Motion Vector Estimation Algorithm Using Mean Pyramid," *IEEE Trans. on Circuits and Systems for Video Technology*, vol. 5, pp.344-351, 1995.
- [13] E. Mémin, and P. Pérez, "Dense Estimation and Object-Based Segmentation of the Optical Flow with Robust Techniques," *IEEE Trans. on Image Processing*, Vol. 7, No. 5, pp. 703-719, 1998.
- [14] J. Y. Lu, K. S. Wu, and J. C. Lin, "Fast Full Search in Motion Estimation by Hierarchical Use of Minkowski's Inequality (HUMI)," *Pattern Recognition*, Vol.31, No. 7, pp. 945-952, 1998.